THE JOURNAL OF PHYSICAL CHEMISTRY C

pubs.acs.org/JPCC Article

Continuum Theory of Electrostatic Correlations at Charged Surfaces

J. Pedro de Souza and Martin Z. Bazant*

Cite This: https://dx.doi.org/10.1021/acs.jpcc.0c01261 Read Online

ACCESS | Metrics & More | Article Recommendations | Supporting Information

ABSTRACT: The standard model for diffuse charge phenomena in colloid science, electrokinetics, and biology is the Poisson−Boltzmann mean-field theory, which breaks down for multivalent ions and large surface charge densities because of electrostatic correlations. In this paper, we formulate a predictive continuum theory of correlated electrolytes based on two extensions of the Bazant−Storey−Kornyshev (BSK) framework: (i) a physical boundary condition enforcing continuity of the Maxwell stress at a charged interface, which upholds the contact theorem for dilute primitive-model electrolytes, and (ii) scaling relationships for the correlation length, for a one-component plasma at a charged plane and around a cylinder, as well as a dilute z:1 electrolyte screening a planar surface. In these cases, the theory accurately reproduces Monte Carlo simulation results from weak to strong coupling, and extensions are possible for more complex models of electrolytes and ionic liquids.

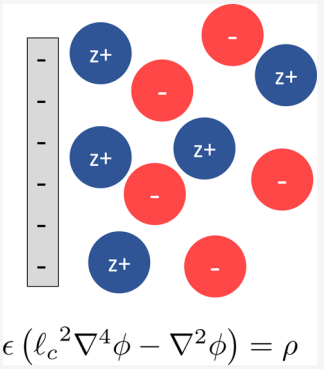

INTRODUCTION

Electrostatic correlations can significantly affect the structure and thermodynamic properties of the electrical double layer,[1,2] resulting in qualitative differences from mean-field Poisson−Boltzmann (PB) theory, such as like-charge attraction[3,4] or over-screening of surface charge. Critical applications in biology, colloids, separations, or electrochemistry rely on or operate in the regime where correlation effects are critical.

Numerous models have been proposed to capture electrostatic correlations, typically with a complicated mathematical structure. Outhwaite derived a modified PB models to account for the fluctuation potential of a single ion interacting with a charged wall.[5] The hypernetted chain approximation and mean spherical approximation closure to the Ornstein−Zernike equation involve solving integral equations involving the direct correlation functions of bulk charged spheres[6−9] for the equilibrium structure. Further work based on classical density functional theory determines equilibrium properties based on the minimization of an integrodifferential free-energy functional. Kierlik and Rosinberg implemented a model (termed the bulk fluid model[10]) which captures correlations based on a perturbative expansion of density with direct correlation functions as an input from the mean spherical approximation.[11] Voukadinova et al. analyzed the accuracy of two other related density functional theories (reference fluid density,[12] functionalized mean spherical approximation,[13] and bulk fluid[11,14]) in comparison to Monte Carlo (MC) simulations, finding the reference fluid density approach to be most accurate.[10] These theories implement the accurate fundamental measure theory functional developed by Rosenfeld to describe excluded volume effects.[15,16] The additional electrostatic interactions beyond mean field are included in the excess free energy separately, without any modification to the mean-field electrostatic part of the free energy.

While these approaches often produce accurate density profiles, they can be involved to implement to a broad range of applications, for different geometries or dynamic problems, especially compared to the classical PB theory. To our knowledge, they also have not yet been shown to recover the correlated behavior of the counterion-only limit for counterions of infinitesimal size. A simpler mathematical structure could help with the application and interpretation of electrostatic correlations to a wider class of problems in physics, including electrokinetics, colloidal interactions, and electrochemical transport/reactions.

Bazant, Storey, and Kornyshev (BSK) proposed a continuum framework to account for the nonlocal dielectric permittivity of ionic liquids resulting from ion−ion correlations[17] with a simple mathematical structure, building on intermediate coupling approximations of Santangelo[18] and Hatlo and Lue[19] for the one-component plasma. The model captures correlations based on expansions in terms of electric field, rather than ion density, in the free-energy functional which leads to a higher-order Poisson equation. In so doing, the electrostatic correlations are included self-consistently in the definition of the electrostatic potential whose gradient determines the electrostatic force on an ion in the diffuse layer.

Received: February 13, 2020
Revised: May 3, 2020
Published: May 5, 2020

https://dx.doi.org/10.1021/acs.jpcc.0c01261
J. Phys. Chem. C XXXX, XXX, XXX−XXX

The BSK theory provides a simple framework to predict charge density oscillations and over-screening phenomena in a variety of electrokinetic, electrochemical, biophysical, and colloidal phenomena in electrolytes and ionic liquids. The equations require a similar level of complexity to solve compared to the PB theory, which allows them to be applied to a broad group of applications. The theory was used to describe electro-smotic[20] and electrophoretic mobility[21] reversals in multivalent and concentrated electrolytes, as well as electroconvective instabilities in ionic liquids.[22] It was also applied to the dynamics[23−27] and electrosorption[28−31] at electrochemical interfaces for ionic liquids and concentrated solvent-in-salt electrolytes, including storage[32] and transport[33] in nanoporous media. Electrostatic correlations have a profound effect on colloidal interactions,[4,34,35] where they can induce like-charge attraction in multivalent electrolytes, also predicted by the BSK theory. The activity and solvation energy of electrolytes at high concentration was also studied including the electrostatic correlation effect[36−40] as well as the extent of ion pairing in confinement.[41] Finally, the electrostatic correlations given by the BSK theory were important in describing the conduction through biological ion channels.[42−46] Despite the numerous applications, fundamental questions remain about the proper boundary conditions and correlation length required to complete the BSK theory.

Here, we show that the appropriate boundary constraint for the higher-order Poisson equation is based on an interfacial stress balance. With corrected boundary conditions, the BSK theory becomes exact in the strong and weak coupling limits for the one-component plasma, and agrees with MC simulations in intermediate coupling. We also suggest scaling relationships for the correlation length without steric constraints in one-component plasma and in multivalent electrolytes, for all the scenarios in Figure 1. We show how

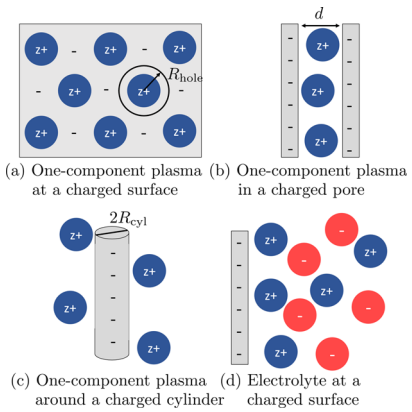

Figure 1. Scenarios considered in the application of the BSK theory.

the correlation length can have a simple physical interpretation based on the correlation hole size of counterions at a charged surface. Although generalizations are possible, we restrict the analysis to a restricted primitive electrolyte with hard, spherical ions of equal size in a constant permittivity, ε and medium and smeared out surface charge density, q_s, and neglect all concentrated-solution effects, so as to isolate electrostatic correlations.

THEORY

The BSK free energy functional is given by

$$G = \int_V d\mathbf{r}\left\{ g + \rho\phi - \frac{\varepsilon}{2}[(\nabla\phi)^2 + l_c^2(\nabla^2\phi)^2 + ...]\right\} + \oint_S d\mathbf{r}_s q_s \phi \quad (1)$$

Here, $g = (H - TS)/V$ is the enthalpy and entropy density, ρ is the charge density, and ϕ is the electrostatic potential. For simplicity, the free energy is truncated after the first correlation contribution, although higher order terms can be considered.[19] While the original authors performed a gradient expansion to arrive at eq 1,[17,20] the mathematical procedure is equivalent to modifying the interaction potential between ions from $U_{\alpha\beta}(r) = z_\alpha z_\beta l_B |r|^{-1}$ to $U_{\alpha\beta}(r) = z_\alpha z_\beta l_B |r|^{-1}(1 - e^{-|r|/l_c})$.[18,25] The modified interaction potential is solved in the mean-field limit. Thus, the BSK theory is a phenomenological correction to PB within the mean-field approximation, by subtracting out interactions with smeared out charges within a correlation length l_c, which should scale as the size of the correlation hole. The modified Poisson equation results by finding the extremal of the functional $(\delta G/\delta\phi = 0)$

$$\varepsilon(l_c^2\nabla^2 - 1)\nabla^2\phi = \rho \quad (2)$$

Equation 2 is a statement of Maxwell's equation, $\nabla\cdot\mathbf{D} = \rho$ where the displacement field is $\mathbf{D} = \hat{\varepsilon}\mathbf{E}$ with a nonlocal permittivity operator $\hat{\varepsilon} = \varepsilon(l_c^2\nabla^2 - 1)$ applied on the electric field, $\mathbf{E} = -\nabla\phi$, in a medium of constant permittivity, ε. PB theory is recovered when $l_c = 0$. Note that the definition of electrostatic potential itself has changed by adding the higher order correlation terms, without violating Maxwell's equation. In other words, the potential that determines the energy of an ion in the double layer must satisfy $\nabla\cdot(\hat{\varepsilon}\mathbf{E}) = \rho$ rather than $\nabla\cdot(\varepsilon\mathbf{E}) = \rho$. In this way, the electrostatic correlation contribution to the electrostatic energy for an ion is included self consistently within the electrostatic framework, rather than being added as additional corrections in the excess chemical potential. An advantage of this approach is that the electrostatic force per unit charge of an ion is captured directly with $\mathbf{E}$, meaning that the diffuse potential ϕ here could be measured experimentally at an electrode (if also accounting for the potential drop in the Stern layer).

The charge density at equilibrium, $\rho = \sum_i z_i e c_i$, will be determined by the constraint that the electrochemical potential for each ion is a constant at equilibrium. The electrochemical potential can be defined as the variation of the Gibbs free energy with respect to concentration,[47] $\mu_i = \delta G/\delta c_i$, or

$$\mu_i = \mu_i^\theta + kT\ln(c_i) + z_i e\phi + \mu_i^{ex} \quad (3)$$

where the first term is a reference value, the second term is the ideal entropy contribution, the third term is the electrostatic potential contribution, and the fourth term is the excess electrochemical potential.

The first open question in applying BSK theory is that of additional boundary conditions, beyond Maxwell's equation $\hat{n}\cdot\mathbf{D} = q_s$. Presumably, the boundary condition must take care of the unaccounted short-range part of $U_{\alpha\beta}$. In the original BSK formulation and all subsequent works, the boundary condition of $\hat{n}\cdot\nabla^3\phi = 0$ was applied, with the justification that the correlation term should disappear at the interface at the distance of closest approach of the ions.[20,21,24−29,33,34,41,42,48,49] The theory provided reasonable agreement to simulation and experimental results for ionic liquids and multivalent electro-

https://dx.doi.org/10.1021/acs.jpcc.0c01261
J. Phys. Chem. C XXXX, XXX, XXX−XXX

lytes. However, the boundary conditions have not yet been proved or validated systematically.

The second open question is the choice of correlation length, which has been arbitrarily set to the Bjerrum length for electrolytes,[17,21] and the ion diameter for ionic liquids.[17] The theory is ultimately very sensitive to the choice of boundary conditions and correlation length. Here, we analyze the boundary condition in terms of a stress balance at the interface and then validate l_c by comparison to MC simulations.

Interfacial Balance. Applying the Gibbs−Duhem equation at constant temperature to the electrolyte and screened surface charges, following ref 50, and neglecting the external electrostatic work done on the system, gives $dP = \sum_i c_i \, d\mu_i$. Taking the gradient in three-dimensional space and applying the definition of the electrochemical potential

$$-\mathbf{f} = \nabla P = kT\sum_i \nabla c_i + \rho\nabla\phi + \sum_i c_i \nabla \mu_i^{ex} \tag{4}$$

where $\mathbf{f}$ is the total thermodynamic force. The first and third terms on the RHS of eq 4 correspond to the gradient of osmotic pressure, $\nabla\Pi$. For an ideal solution, $\mu_i^{ex} = 0$. The gradient of the defined thermodynamic pressure is equivalent to the divergence of the total stress tensor of the electrolyte system, $\mathbf{f} = \nabla\cdot\tau$. The total stress tensor is composed of an osmotic pressure component, Π and a Maxwell stress tensor, τ_e, such that $\tau = -\Pi\mathbf{I} + \tau_e$. The component of interest in this analysis, τ_e, can be defined by

$$\nabla\cdot\tau_e = \rho\mathbf{E} = \nabla\cdot(\hat{\varepsilon}\mathbf{E})\mathbf{E} \tag{5}$$

in a constant ε medium. Plugging in for the charge density using the BSK eq 2 and performing integration by parts, one arrives at an expression for the Maxwell stress tensor for a fluid with a nonlocal permittivity

$$\tau_e = \varepsilon\mathbf{E}\mathbf{E} - \frac{1}{2}\varepsilon\mathbf{E}^2\mathbf{I} + \varepsilon l_c^2\Big[(\mathbf{E}\cdot\nabla^2\mathbf{E})\mathbf{I} - \mathbf{E}(\nabla^2\mathbf{E}) - (\nabla^2\mathbf{E})\mathbf{E} + \frac{1}{2}(\nabla\cdot\mathbf{E})^2\mathbf{I}\Big] \tag{6}$$

as derived in the Supporting Information. Although the above equation was derived for constant ε and l_c, the expression is identical if these parameters vary. For varying ε or l_c, the Korteweg−Helmholtz force density must be included in the electrostatic stress[51]

$$\nabla\cdot\tau_e = \rho\mathbf{E} - \frac{1}{2}\mathbf{E}^2\nabla\varepsilon + \frac{1}{2}(\nabla\cdot\mathbf{E})^2\nabla(\varepsilon l_c^2) \tag{7}$$

Within the distance of closest approach of the ions to the surface, correlations cannot affect the value of the Maxwell stress at the surface, $\tau_{e,surf}$, generated by the surface charge density. The mechanical equilibrium problem therefore requires continuity in the electrostatic stress tensor evaluated in the solution and at the surface

$$\tau_e - \tau_{e,surf} = 0 \tag{8}$$

At a uniformly charged, flat surface without a dielectric jump, the Maxwell stress tensor is simply $\tau_{e,surf} = q_s^2/(2\varepsilon)\hat{n}\hat{n}$, while the Maxwell stress tensor in the electrolyte is given by eq 6. Equating these two expressions, and substituting in $\hat{n}\cdot\mathbf{D} = q_s$, we arrive at a final boundary for a potential varying in one coordinate direction

$$\hat{n}\cdot l_c\nabla^3\phi = \nabla^2\phi|_S \tag{9}$$

applied at the distance of closest approach of the ion with the wall.

The method amounts to applying the contact theorem to the correlated electrolyte in the absence of correlations, shown below for $\mu_i^{ex} = 0$ at a flat electrode with constant charge density without a dielectric jump[52,53]

$$P = -\frac{q_s^2}{2\varepsilon} + kT\sum_i c_i\Big|_S = -\hat{n}\cdot\tau_e\cdot\hat{n} + kT\sum_i c_i\Big|_S \tag{10}$$

The contact theorem is a statement of mechanical equilibrium, where the repulsive osmotic pressure contribution is balanced by the electrostatic attraction from the Maxwell stress. Without the constraint from eq 8, the BSK theory does not obey this simple relationship which should be valid even for dilute electrolytes in the primitive model.[54−56] The procedure of ensuring continuity in the Maxwell stress can be repeated for any higher order $\hat{\varepsilon}$ by equating the τ_e at successive orders of derivatives. The condition in eq 8 is also applicable to any extended electrolyte mean-field theory with arbitrary models of concentrated solution activity and solvent polarizability, including interactions with a soft wall. The approach may even be extended to media with nonlocal dielectric constant $\hat{\varepsilon}$ driven by solvent polarization.[57,58]

Correlation Length Scaling. At highly charged surfaces, the charge−charge correlations are dominated by the mutual repulsion of counterions at the interface, as demonstrated in the schematic in Figure 1a. The size of a correlation hole of counterions forming a Wigner crystal is characterized by a length scale R_{hole}

$$R_{hole} = \left(\frac{1}{6}\right)^{1/4}\left(\frac{ze}{q_s}\right)^{1/2} \tag{11}$$

where z is the ion valency and e is an elementary charge. For this work, we assume that the correlation length scales as the size of a correlation hole, determined by the surface charge density

$$l_c = \alpha R_{hole} \tag{12}$$

with one parameter α, which is considered to be a constant. We will demonstrate that the fitted scaling with $\alpha = 0.50$ works well from the limit of zero reservoir concentration (one-component plasma) to more concentrated electrolytes. At high concentration or at low surface charge densities, this scaling argument breaks down, and the other length scales might dominate in the correlation length. For example, if the surface charge tends to zero, then the charge−charge correlations will be dominated by the Bjerrum length and characteristic mean spacing between ions given by the bulk concentration. At very large charge densities and for large ion sizes, where R_{hole} becomes comparable to a, the ion diameter, the ion size can dominate in determining the charge−charge correlations due to over-crowding effects. Also, if other length scales are introduced, such as surface curvature, the correlation length between ions can also be affected, as demonstrated with the one-component plasma around a thin charged cylinder.

In the Supporting Information, the nonarbitrary scaling of the correlation length is investigated by comparison to grand canonical MC (GCMC) simulations from ref 59 for a z:1 electrolyte. Using the Buckingham-Π theorem, we know that the correlation length is related to functions of dimensionless

https://dx.doi.org/10.1021/acs.jpcc.0c01261
J. Phys. Chem. C XXXX, XXX, XXX−XXX

ratios of other length scales of the problem. At small or large values of these dimensionless ratios, the functional dependence becomes a power law relationship by expanding the individual functions, which we assume in this work. Here, we choose four length scales from which we can construct three dimensionless groups from: the correlation length, l_c, the Gouy−Chapman length, l_{GC}, the Bjerrum length, $z^2 l_B$, and the Debye length λ_D, such that the power law relationship can be expressed as

$$\delta_c = \frac{l_c}{\lambda_D} = \alpha_2 \left(\frac{z^2 l_B}{l_{GC}}\right)^{\alpha_3} \left(\frac{z^2 l_B}{\lambda_D}\right)^{\alpha_4} \tag{13}$$

where δ_c is the correlation length l_c divided by the Debye length. The definitions and meanings of the different length scales will be included in the Results and Discussion section as they appear in the mathematical framework.

The correlation length scaling that arises from the fitting procedure to the MC data is given by

$$l_c \sim {l_B}^{1/4} (q_s/e)^{-1/8} {C_{ref}}^{-1/6} \tag{14}$$

with a fitted scale of

$$\delta_c = 0.35 \left(\frac{z^2 l_B}{l_{GC}}\right)^{-1/8} \left(\frac{z^2 l_B}{\lambda_D}\right)^{2/3} \tag{15}$$

Note that the fitted exponents are expressed in terms of fractions to emphasize their relationship to the intrinsic length scales in the system.

A detailed investigation of how correlations are affected as a function of surface charge density, ion valency, concentration, ion size, and surface curvature could motivate a more nuanced scaling of the correlation length, based on direct analysis of the charge−charge correlation function, including variations in the correlation length as a function of the distance from a charged surface. For example, the fitted correlation length relationship in eq 15 does not return the correlation length for the counterion only system in the limit of zero ion concentration. In this work, we isolate the electrostatic correlation effects for a dilute electrolyte at highly charged surfaces. For the purposes of the analysis in the main text, we will assume the correlation length to be $l_c = 0.50 R_{hole}$ for all of the scenarios investigated in Figure 1. For the results with the fitted correlation length scaling in 15, one can refer to the Supporting Information.

RESULTS AND DISCUSSION

One-Component Plasma. Considering a system of point-like counterions neutralizing a uniformly charged surface, the importance of correlations is governed by a coupling constant

$$\Xi = 2\pi z^3 {l_B}^2 q_s/e \tag{16}$$

which is a measure of the correlation hole size, R_{hole}, compared to the characteristic ion distance from the surface, the Gouy−Chapman length

$$l_{GC} = e(2\pi z l_B q_s)^{-1} \tag{17}$$

such that $\Xi \sim {R_{hole}}^2/{l_{GC}}^2$. Note that the Bjerrum length, l_B is defined as the distance at which two unit charges experience an electrostatic energy equal to the thermal energy

$$l_B = \frac{e^2}{4\pi\varepsilon k_B T} \tag{18}$$

In the weak coupling limit ($\Xi \ll 1$), PB theory is valid. In the strong coupling limit ($\Xi \gg 1$), counterions interact with the electric potential created by the surface because ion−surface interactions dominate.[2,54,55,60,61]

Now we consider applying the mechanical constraint, starting with the one-component plasma of infinitesimally small size with $\mu^{ex} = 0$. The one-component plasma consists of a single mobile ionic species which neutralizes the charge of a smeared out surface charge density. We can nondimensionalize lengths with the Gouy−Chapman length, the potential by the thermal voltage for the counterion, $\phi_0 = kT/ze$, and the charge density by $\rho_0 = 2\pi l_B {q_s}^2 e^{-1}$. Here, we assume that the correlation length scales with the size of a correlation hole at the surface, $\delta_c = l_c/l_{GC} = \alpha_0\sqrt{\Xi}$ Using $\sim$ to denote non-dimensionalized variables

$${\alpha_0}^2 \Xi \tilde{\nabla}^4 \tilde{\phi} - \tilde{\nabla}^2 \tilde{\phi} = 2\tilde{\rho} = 2e^{-\tilde{\phi}} \tag{19}$$

with boundary conditions of

$$\hat{n}\cdot({\alpha_0}^2 \Xi \tilde{\nabla}^3 \tilde{\phi} - \tilde{\nabla}\tilde{\phi}) = -2$$
$$\hat{n}\cdot\alpha_0\sqrt{\Xi}\tilde{\nabla}^3\tilde{\phi} = \tilde{\nabla}^2\tilde{\phi} \tag{20}$$

at $\tilde{x} = 0$, where $\alpha_0 = 1.36\alpha$ is an order one constant proportional to α. Therefore, the importance of the higher order derivative is governed by the coupling parameter, Ξ.

The solution to these equations is compared to the results of MC simulations in Figure 2 for a one-component plasma

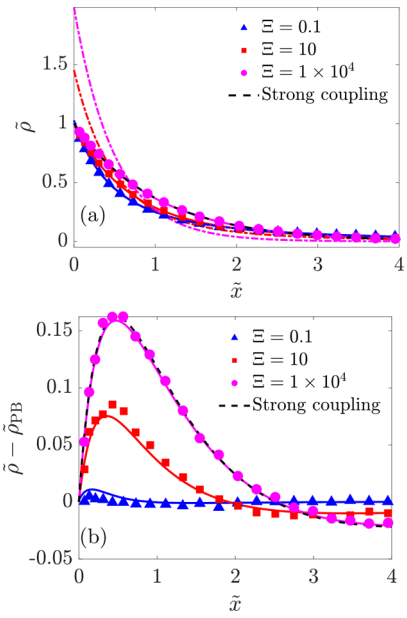

Figure 2. Isolated charged plate. BSK theory for one-component plasma compared to MC simulations from ref 54 with $\alpha = 0.50$ for counterions screening a charged isolated surface. The solid lines are the predictions of the BSK theory with the boundary condition of $\hat{n}\cdot l_c\nabla^3\phi = \nabla^2\phi|_S$, the dashed-dotted lines are the predictions of the BSK theory with the boundary condition of $\hat{n}\cdot l_c\nabla^3\phi = 0$, and the markers are from the MC simulations. Strong coupling limits are plotted as black dashed lines. (a) Charge density is plotted as a function of distance from an isolated surface. (b) Charge density difference relative to the solution to the PB theory as a function of distance from an isolated surface.

https://dx.doi.org/10.1021/acs.jpcc.0c01261
J. Phys. Chem. C XXXX, XXX, XXX−XXX

screening a plane of charge. The BSK theory reproduces the behavior of the one-component plasma from weak coupling, in intermediate coupling, and matches the strong coupling limit with $\alpha = 0.50$. Furthermore, the BSK theory with the boundary condition of $\hat{n}\cdot\nabla^3\phi = 0$, represented by the dashed-dotted lines in Figure 2a, does not accurately represent the data at intermediate or strong coupling.

We can also consider the one-component plasma between two charged surfaces of equal charge density with the same sign, confining the counterions in a gap of dimensionless distance $\tilde{d}$, as shown in Figure 3a. In Figure 3b, the pressure is

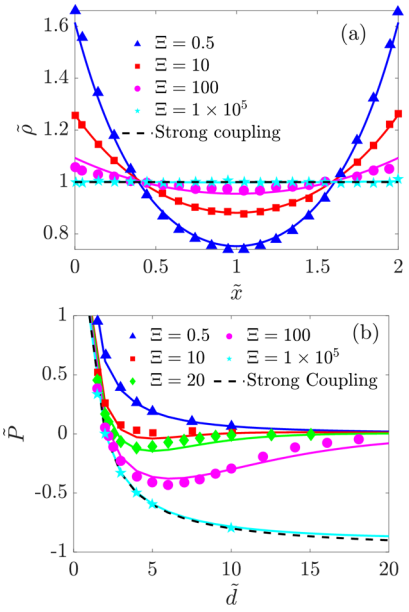

Figure 3. Confined geometry. BSK theory for one-component plasma compared to MC simulations of counterions between two like charged surfaces from ref 54 with $\alpha = 0.50$. The solid lines are the predictions of the BSK theory, and the markers are from the MC simulations. Strong coupling limits are plotted as dashed lines. (a) Charge density is plotted between two surfaces with separation $\tilde{d} = 2$. (b) Pressure is calculated as a function of separation distance between the two plates. As the coupling increases, the pressures between the like-charged surfaces become attractive (negative) rather than repulsive (positive). The dimensionless pressure is $\tilde{P} = Pe^2/(2\pi l_B q_s^2)$.

plotted as a function of separation distances between two charged surfaces with different coupling parameters, using eq 8 and using the same value for α. The BSK theory again provides good agreement with the results of the MC simulations at all the coupling parameters.

Another critical question is the validity of eq 8 at a curved interface. The simplest model system to test the hypothesis is the one-component plasma surrounding a charged cylinder of radius $\xi = R_{cyl}/l_{GC}$ at infinite dilution, corresponding to a cylindrical cell with outer radius $R_{out} \to \infty$. As shown in Figure 4 and Supporting Information Figure S1, the BSK equation reproduces the results of the weak and strong coupling limits correctly, by applying the boundary condition in eq 20 at $\tilde{r} = \xi$. However, similar to the strong coupling expansion of ref 63, the theory does not correctly describe the renormalization of charge arising from Manning condensation in the needle limit, where a fraction $f = 1 - 1/\xi$ of the charge is "condensed" onto cylinder.[64] The charge density must be multiplied by this

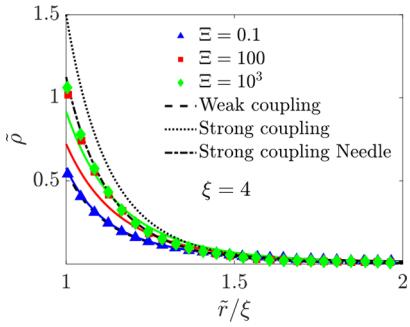

Figure 4. Cylindrical geometry. BSK theory for one-component plasma compared to MC simulations from ref 62 using $\alpha = 0.50$ for the counterion density around a charged cylinder for $\xi = 4$. The solid lines are the results of applying eq 19 and the markers are the MC simulation results from ref 62. The weak coupling, strong coupling, and renormalized strong coupling needle limits are plotted.[62]

fraction, f, in order to match the strong coupling expansion taking into account the charge renormalization in the needle limit.[62,65] The smaller the radius of curvature, the more likely that the configuration of correlated ions is influenced by curvature. In the "needle limit," where $\sqrt{\Xi}/\xi \gg 1$, ions are distributed in a nearly linear fashion along the cylindrical backbone with spacing scaling as $\tilde{a} \sim \Xi/\xi$, which may also be the relevant scaling for the correlation length in this regime rather than $\sqrt{\Xi}$. Supporting Information Figures S1 and S2 show the results choosing $\delta_c = \Xi/\xi$, but the counterion condensation transition is still not captured.

Electrolytes. A more useful and relevant application of the BSK theory is to describe the distribution of charges in electrolytes and ionic liquids, as was originally proposed. Here, we focus on the dilute electrolyte limit, to isolate electrostatic correlations directly, without complications from overcrowding.

If the BSK equation for a z:1 electrolyte with salt concentration C_{ref} is nondimensionalized with the thermal voltage $\tilde{\phi} = (e\phi)/(kT)$ and the Debye length

$$\lambda_D = \sqrt{\frac{\varepsilon kT}{(z^2 + z)e^2 C_{ref}}} \tag{21}$$

$\tilde{\nabla} = \lambda_D \nabla$ and $\delta_c = l_c/\lambda_D$ the BSK equation becomes

$$\delta_c^2 \tilde{\nabla}^4 \tilde{\phi} - \tilde{\nabla}^2 \tilde{\phi} = \tilde{\rho} = \frac{ze^{-z\tilde{\phi}} - ze^{\tilde{\phi}}}{z^2 + z} \tag{22}$$

The boundary conditions are similarly modified to

$$\hat{n}\cdot(\delta_c^2 \tilde{\nabla}^3 \tilde{\phi} - \tilde{\nabla}\tilde{\phi}) = \tilde{q}_s$$
$$\hat{n}\cdot\delta_c \tilde{\nabla}^3 \tilde{\phi} = \tilde{\nabla}^2 \tilde{\phi} \tag{23}$$

The agreement of the predicted charge density profiles from eq 22 with the GCMC data is very good, as exhibited in Figure 5 for a 0.1 M 2:1 electrolyte. In the Supporting Information, the results are expanded to a more complete set of comparisons with simulations. It is seen with $l_c = 0.50R_{hole}$ or with l_c determined by eq 15 that the BSK theory can correct the PB charge density profiles, including an overscreening transition. Larger errors from the BSK theory are incurred at large concentration, where the current assumption of $\mu_i^{ex} = 0$ breaks down.

https://dx.doi.org/10.1021/acs.jpcc.0c01261
J. Phys. Chem. C XXXX, XXX, XXX−XXX

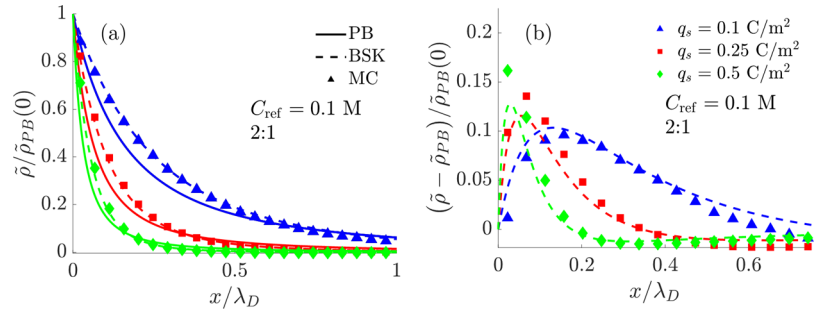

Figure 5. Electrolyte at an isolated plate. BSK theory for an electrolyte solution compared to MC simulations[59] of multivalent electrolytes with α = 0.50. (a) Example of the charge density profile for a 2:1 electrolyte at 0.1 M concentration compared to the GCMC simulations and PB theory. (b) Difference between the predictions of the BSK theory and the simulations from PB theory predictions.

One implication of the boundary condition is that the differential capacitance for $l_c = 0$ is equivalent to the case of $l_c \neq 0$ if $\mu_i^{ex} = 0$. Therefore, the differential capacitance for the correlated, dilute electrolyte is given by the traditional Gouy–Chapman equation

$$C_D = \frac{\varepsilon}{\lambda_D}\cosh\left(\frac{\tilde{\phi}_D}{2}\right) \tag{24}$$

in stark contrast to the original work in the limit of $\mu_i^{ex} = 0$.[17,20] It would be interesting to explore the implications of the boundary condition on electrokinetic reversals, electrochemical interfaces, biological channels, or colloidal phenomena.[20,21,24−29,33,34,41,42,48] For example, the DLVO theory of colloidal interactions can be modified to include attractive correlation effects.[4]

Further Extensions of the Theory. *Charged Dielectric Interfaces.* Note that the Maxwell stress condition (eq 6) has only been stated without a dielectric jump. The stress condition may need further validation at a dielectric interface. A more general statement of matching the Maxwell stress with and without correlations might be given by a jump condition between the two media

$$\hat{n}\cdot[\tau_{e,1} - \tau_{e,2}] = \hat{n}\cdot[\tau_{e,1} - \tau_{e,2}]_{l_c=0} \tag{25}$$

For a uniformly charged, flat interface without a dielectric jump, $\tau_{e,2} = 0$, so the RHS of the above equation reduces to $\hat{n}\cdot[\tau_{e,1} - \tau_{e,2}]_{l_c=0} = \frac{q_s^2}{2\varepsilon_1}\hat{n}$.

Concentrated Electrolytes and Ionic Liquids. The present analysis attempts to isolate the effect of ion correlations in a dilute electrolyte. Ion size effects, particularly for $a/\lambda_D > 1$ will require further validation to properly account for correlations guided by ion size combined with electrostatics. A nonlocal free-energy functional might be necessary to capture the size correlations in concentrated solutions,[16,66] in conjunction with electrostatic correlations. Short-range bulk correlations[67] are not captured in this theory. Furthermore, if surface charges are discrete rather than smeared out, the contact condition may change,[68] although the boundary condition derived here could be applied to such charge density distributions. For an arbitrary mixture of ions with different valency, the effective correlation length will depend upon correlations between each pair of species, although the correlations at high surface charge density will still be dominated by the most highly charged counterion.

CONCLUSIONS

The phenomenological BSK theory describes nonlocal, discrete correlation effects with a higher-order, local, continuum description of the free energy quite well. The remarkable agreement of the theory with the one-component plasma and primitive model electrolyte suggest that higher-order, continuum equations can properly account for correlation effects, as long as the appropriate constraints are imposed at boundaries. The formalism used here could be extended to the ionic liquid limit, although ion pairing, short-range nonelectrostatic correlations, and "spin glass" ordering[69] might preclude a simple continuum description. Further modifications are needed to capture the long-range screening exhibited in ionic liquids and concentrated electrolytes,[70] as well as density oscillations expected in overcrowded systems.[16] Even so, the BSK theory captures important features of electrostatic correlations, including like-charge attraction and overscreening, driven by electrostatic interactions of spatially correlated counterions. Furthermore, unlike many previous approaches, all of the electrostatic forces are contained self-consistently within the electrostatic potential, ϕ. Detailed analysis of experimental data is needed to determine the competing effects of surface adsorption reactions modifying fixed surface charge[71] or the overscreening/like-charge attraction effects modeled by the BSK theory.[4]

ASSOCIATED CONTENT

Supporting Information

The Supporting Information is available free of charge at https://pubs.acs.org/doi/10.1021/acs.jpcc.0c01261.

Derivation of the Maxwell stress, additional results of counterions around a cylinder, and comprehensive comparison to a simulation data set (PDF)

AUTHOR INFORMATION

Corresponding Author

Martin Z. Bazant − *Department of Chemical Engineering and Department of Mathematics, Massachusetts Institute of Technology, Cambridge, Massachusetts 02142, United States;* orcid.org/0000-0002-8200-4501; Phone: 617-324-2036; Email: bazant@mit.edu

Author

J. Pedro de Souza − *Department of Chemical Engineering, Massachusetts Institute of Technology, Cambridge, Massachusetts 02142, United States*

Complete contact information is available at:

https://dx.doi.org/10.1021/acs.jpcc.0c01261
J. Phys. Chem. C XXXX, XXX, XXX−XXX

https://pubs.acs.org/10.1021/acs.jpcc.0c01261

Notes

The authors declare no competing financial interest.

■ ACKNOWLEDGMENTS

This work was supported by an Amar G. Bose Research Grant (electrolyte calculations) and the Center for Enhanced Nanofluid Transport an Energy Frontier Research Center funded by the U.S. Department of Energy, Office of Science, Basic Energy Sciences under award no. DE-SC0019112 (one-component plasma calculations). J.P.d.S. is also supported by the National Science Foundation Graduate Research Fellowship under grant no. 1122374. J.P.d.S. would like to acknowledge useful discussions with Michael McEldrew, Amir Levy, Tingtao Zhou, Dimitrios Fraggedakis, and Mohammad Mirzadeh.

■ REFERENCES

(1) Levin, Y. Electrostatic correlations: from plasma to biology. *Rep. Prog. Phys.* **2002**, *65*, 1577−1632.
(2) Grosberg, A. Y.; Nguyen, T. T.; Shklovskii, B. I. Colloquium: the physics of charge inversion in chemical and biological systems. *Rev. Mod. Phys.* **2002**, *74*, 329.
(3) Pellenq, R. J.-M.; Caillol, J. M.; Delville, A. Electrostatic Attraction between Two Charged Surfaces: A (N,V,T) Monte Carlo Simulation. *J. Phys. Chem. B* **1997**, *101*, 8584−8594.
(4) Misra, R. P.; de Souza, J. P.; Blankschtein, D.; Bazant, M. Z. Theory of surface forces in multivalent electrolytes. *Langmuir* **2019**, *35*, 11550−11565.
(5) Outhwaite, C. W.; Bhuiyan, L. B. An improved modified Poisson-Boltzmann equation in electric-double-layer theory. *J. Chem. Soc., Faraday Trans. 2* **1983**, *79*, 707−718.
(6) Henderson, D.; Blum, L. Some exact results and the application of the mean spherical approximation to charged hard spheres near a charged hard wall. *J. Chem. Phys.* **1978**, *69*, 5441−5449.
(7) Henderson, D.; Blum, L.; Smith, W. R. Application of the hypernetted chain approximation to the electric double layer at a charged planar interface. *Chem. Phys. Lett.* **1979**, *63*, 381−383.
(8) Lozada-Cassou, M.; Saavedra-Barrera, R.; Henderson, D. The application of the hypernetted chain approximation to the electrical double layer: Comparison with Monte Carlo results for symmetric salts. *J. Chem. Phys.* **1982**, *77*, 5150−5156.
(9) Kjellander, R.; Åessonn, T.; Jönsson, B.; Marčelja, S. Double layer interactions in mono-and divalent electrolytes: A comparison of the anisotropic HNC theory and Monte Carlo simulations. *J. Chem. Phys.* **1992**, *97*, 1424−1431.
(10) Voukadinova, A.; Valiskó, M.; Gillespie, D. Assessing the accuracy of three classical density functional theories of the electrical double layer. *Phys. Rev. E* **2018**, *98*, 012116.
(11) Kierlik, E.; Rosinberg, M. L. Density-functional theory for inhomogeneous fluids: adsorption of binary mixtures. *Phys. Rev. A* **1991**, *44*, 5025.
(12) Gillespie, D.; Nonner, W.; Eisenberg, R. S. Coupling Poisson Nernst Planck and density functional theory to calculate ion flux. *J. Phys.: Condens. Matter* **2002**, *14*, 12129.
(13) Roth, R.; Gillespie, D. Shells of charge: a density functional theory for charged hard spheres. *J. Phys.: Condens. Matter* **2016**, *28*, 244006.
(14) Rosenfeld, Y. Free energy model for inhomogeneous fluid mixtures: Yukawa-charged hard spheres, general interactions, and plasmas. *J. Chem. Phys.* **1993**, *98*, 8126−8148.
(15) Rosenfeld, Y. Free-energy model for the inhomogeneous hard-sphere fluid mixture and density-functional theory of freezing. *Phys. Rev. Lett.* **1989**, *63*, 980.
(16) Roth, R. Fundamental measure theory for hard-sphere mixtures: a review. *J. Phys.: Condens. Matter* **2010**, *22*, 063102.
(17) Bazant, M. Z.; Storey, B. D.; Kornyshev, A. A. Double layer in ionic liquids: overscreening versus crowding. *Phys. Rev. Lett.* **2011**, *106*, 046102.
(18) Santangelo, C. D. Computing counterion densities at intermediate coupling. *Phys. Rev. E: Stat., Nonlinear, Soft Matter Phys.* **2006**, *73*, 041512.
(19) Hatlo, M. M.; Lue, L. Electrostatic interactions of charged bodies from the weak- to the strong-coupling regime. *Europhys. Lett.* **2010**, *89*, 25002.
(20) Storey, B. D.; Bazant, M. Z. Effects of electrostatic correlations on electrokinetic phenomena. *Phys. Rev. E: Stat., Nonlinear, Soft Matter Phys.* **2012**, *86*, 056303.
(21) Stout, R. F.; Khair, A. S. A continuum approach to predicting electrophoretic mobility reversals. *J. Fluid Mech.* **2014**, *752*, R1.
(22) Wang, C.; Bao, J.; Pan, W.; Sun, X. Modeling electrokinetics in ionic liquids. *Electrophoresis* **2017**, *38*, 1693−1705.
(23) Zhao, H. Diffuse-charge dynamics of ionic liquids in electrochemical systems. *Phys. Rev. E: Stat., Nonlinear, Soft Matter Phys.* **2011**, *84*, 051504.
(24) Jiang, X.; Huang, J.; Zhao, H.; Sumpter, B. G.; Qiao, R. Dynamics of electrical double layer formation in room-temperature ionic liquids under constant-current charging conditions. *J. Phys.: Condens. Matter* **2014**, *26*, 284109.
(25) Lee, A. A.; Kondrat, S.; Vella, D.; Goriely, A. Dynamics of Ion Transport in Ionic Liquids. *Phys. Rev. Lett.* **2015**, *115*, 106101.
(26) Alijó, P. H. R.; Tavares, F. W.; Biscaia, E. C., Jr.; Secchi, A. R. Effects of electrostatic correlations on ion dynamics in alternating current voltages. *Electrochim. Acta* **2015**, *152*, 84−92.
(27) Alidoosti, E.; Zhao, H. On the impact of electrostatic correlations on the double-layer polarization of a spherical particle in an alternating current field. *Langmuir* **2018**, *34*, 5592−5599.
(28) Lee, D. W.; Im, D. J.; Kang, I. S. Electric Double Layer at the Interface of Ionic Liquid-Dielectric Liquid under Electric Field. *Langmuir* **2013**, *29*, 1875−1884.
(29) McEldrew, M.; Goodwin, Z. A. H.; Kornyshev, A. A.; Bazant, M. Z. Theory of the double layer in water-in-salt electrolytes. *J. Phys. Chem. Lett.* **2018**, *9*, 5840−5846.
(30) Shalabi, A.; Daniels, L.; Scott, M.; Mišković, Z. L. Differential capacitance of ionic liquid interface with graphene: The effects of correlation and finite size of ions. *Electrochim. Acta* **2019**, *319*, 423−434.
(31) Xie, D.; Jiang, Y. Nonlocal Poisson-Fermi double-layer models: Effects of nonuniform ion sizes on double-layer structure. *Phys. Rev. E* **2018**, *97*, 052610.
(32) Yang, Y. D.; Moon, G. J.; Oh, J. M.; Kang, I. S. Discrete and continuum analyses of confinement effects of an ionic liquid on the EDL structure and the pressure acting on the wall. *J. Phys. Chem. C* **2019**, *123*, 2516−2525.
(33) Jiang, X.; Liu, Y.; Qiao, R. Current rectification for transport of room-temperature ionic liquids through conical nanopores. *J. Phys. Chem. C* **2016**, *120*, 4629−4637.
(34) Moon, G. J.; Ahn, M. M.; Kang, I. S. Osmotic pressure of ionic liquids in an electric double layer: Prediction based on a continuum model. *Phys. Rev. E: Stat., Nonlinear, Soft Matter Phys.* **2015**, *92*, 063020.
(35) Santos, M. S.; Biscaia, E. C., Jr.; Tavares, F. W. Effect of electrostatic correlations on micelle formation. *Colloids Surf., A* **2017**, *533*, 169−178.
(36) Liu, J.-L.; Eisenberg, B. Poisson−Fermi model of single ion activities in aqueous solutions. *Chem. Phys. Lett.* **2015**, *637*, 1−6.
(37) Schlumpberger, S.; Bazant, M. Z. Simple theory of ionic activity in concentrated electrolytes. **2017**, arXiv:1709.03106. arXiv preprint.
(38) Liu, J.-L.; Eisenberg, B. Poisson-Fermi modeling of ion activities in aqueous single and mixed electrolyte solutions at variable temperature. *J. Chem. Phys.* **2018**, *148*, 054501.
(39) Nakamura, I. Effects of dielectric inhomogeneity and electrostatic correlation on the solvation energy of ions in liquids. *J. Phys. Chem. B* **2018**, *122*, 6064−6071.

(40) Liu, J.-L.; Li, C.-L. A generalized Debye−Hückel theory of electrolyte solutions. *AIP Adv.* **2019**, *9*, 015214.
(41) Huang, J. Confinement induced dilution: Electrostatic screening length anomaly in concentrated electrolytes in confined space. *J. Phys. Chem. C* **2018**, *122*, 3428−3433.
(42) Liu, J.-L. Numerical methods for the Poisson−Fermi equation in electrolytes. *J. Comput. Phys.* **2013**, *247*, 88−99.
(43) Liu, J.-L.; Eisenberg, B. Correlated Ions in a Calcium Channel Model: A Poisson−Fermi Theory. *J. Phys. Chem. B* **2013**, *117*, 12051−12058.
(44) Liu, J.-L.; Eisenberg, B. Poisson-Nernst-Planck-Fermi theory for modeling biological ion channels. *J. Chem. Phys.* **2014**, *141*, 22D532.
(45) Liu, J.-L.; Eisenberg, B. Analytical models of calcium binding in a calcium channel. *J. Chem. Phys.* **2014**, *141*, 075102.
(46) Liu, J.-L.; Eisenberg, B. Numerical methods for a Poisson-Nernst-Planck-Fermi model of biological ion channels. *Phys. Rev. E: Stat., Nonlinear, Soft Matter Phys.* **2015**, *92*, 012711.
(47) Bazant, M. Z. Theory of chemical kinetics and charge transfer based on nonequilibrium thermodynamics. *Acc. Chem. Res.* **2013**, *46*, 1144−1160.
(48) dos Santos, A. P.; Diehl, A.; Levin, Y. Electrostatic correlations in colloidal suspensions: Density profiles and effective charges beyond the Poisson−Boltzmann theory. *J. Chem. Phys.* **2009**, *130*, 124110.
(49) Gupta, A.; Stone, H. A. Electrical double layers: Effects of asymmetry in electrolyte valence on steric effects, dielectric decrement, and ion−ion correlations. *Langmuir* **2018**, *34*, 11971−11985.
(50) Bazant, M. Z.; Kilic, M. S.; Storey, B. D.; Ajdari, A. Towards an understanding of induced-charge electrokinetics at large applied voltages in concentrated solutions. *Adv. Colloid Interface Sci.* **2009**, *152*, 48−88.
(51) Woodson, H. H.; Melcher, J. R. *Electromechanical Dynamics*; Wiley, 1968.
(52) Alawneh, M.; Henderson, D. Monte Carlo simulation of the double layer at an electrode including the effect of a dielectric boundary. *Mol. Simul.* **2007**, *33*, 541−547.
(53) Henderson, D.; Blum, L.; Lebowitz, J. L. An exact formula for the contact value of the density profile of a system of charged hard spheres near a charged wall. *J. Electroanal. Chem. Interfacial Electrochem.* **1979**, *102*, 315−319.
(54) Moreira, A. G.; Netz, R. R. Simulations of counterions at charged plates. *Eur. Phys. J. E: Soft Matter Biol. Phys.* **2002**, *8*, 33−58.
(55) Burak, Y.; Andelman, D.; Orland, H. Test-charge theory for the electric double layer. *Phys. Rev. E: Stat., Nonlinear, Soft Matter Phys.* **2004**, *70*, 016102.
(56) Carnie, S. L.; Chan, D. Y. C. Ionic adsorption from a primitive model electrolyte-nonlinear treatment. *J. Chem. Phys.* **1981**, *75*, 3485−3494.
(57) Kornyshev, A. A.; Rubinshtein, A. I.; Vorotyntsev, M. A. Model nonlocal electrostatics. I. *J. Phys. C: Solid State Phys.* **1978**, *11*, 3307.
(58) Kornyshev, A. A. Nonlocal screening of ions in a structurized polar liquid - new aspects of solvent description in electrolyte theory. *Electrochim. Acta* **1981**, *26*, 1−20.
(59) Valiskó, M.; Kristóf, T.; Gillespie, D.; Boda, D. A systematic Monte Carlo simulation study of the primitive model planar electrical double layer over an extended range of concentrations, electrode charges, cation diameters and valences. *AIP Adv.* **2018**, *8*, 025320.
(60) Palaia, I.; Trulsson, M.; Šamaj, L.; Trizac, E. A correlation-hole approach to the electric double layer with counter-ions only. *Mol. Phys.* **2018**, *116*, 3134−3146.
(61) Šamaj, L.; Trulsson, M.; Trizac, E. Strong-coupling theory of counterions between symmetrically charged walls: from crystal to fluid phases. *Soft Matter* **2018**, *14*, 4040−4052.
(62) Mallarino, J. P.; Téllez, G.; Trizac, E. Counterion density profile around charged cylinders: the strong-coupling needle limit. *J. Phys. Chem. B* **2013**, *117*, 12702−12716.
(63) Naji, A.; Netz, R. R. Counterions at charged cylinders: criticality and universality beyond mean-field theory. *Phys. Rev. Lett.* **2005**, *95*, 185703.
(64) Manning, G. S. Limiting laws and counterion condensation in polyelectrolyte solutions I. Colligative properties. *J. Chem. Phys.* **1969**, *51*, 924−933.
(65) Cha, M.; Yi, J.; Kim, Y. W. Hidden criticality of counterion condensation near a charged cylinder. *Sci. Rep.* **2017**, *7*, 10551.
(66) Gillespie, D. A review of steric interactions of ions: Why some theories succeed and others fail to account for ion size. *Microfluid. Nanofluid.* **2015**, *18*, 717−738.
(67) Goodwin, Z. A. H.; Feng, G.; Kornyshev, A. A. Mean-field theory of electrical double layer in ionic liquids with account of short-range correlations. *Electrochim. Acta* **2017**, *225*, 190−197.
(68) Moreira, A. G.; Netz, R. R. Counterions at charge-modulated substrates. *Europhys. Lett.* **2002**, *57*, 911.
(69) Levy, A.; McEldrew, M.; Bazant, M. Z. Spin-glass charge ordering in ionic liquids. *Phys. Rev. Mater.* **2019**, *3*, 055606.
(70) Smith, A. M.; Lee, A. A.; Perkin, S. The electrostatic screening length in concentrated electrolytes increases with concentration. *J. Phys. Chem. Lett.* **2016**, *7*, 2157−2163.
(71) Mugele, F.; Bera, B.; Cavalli, A.; Siretanu, I.; Maestro, A.; Duits, M.; Cohen-Stuart, M.; Van Den Ende, D.; Stocker, I.; Collins, I. Ion adsorption-induced wetting transition in oil-water-mineral systems. *Sci. Rep.* **2015**, *5*, 10519.

https://dx.doi.org/10.1021/acs.jpcc.0c01261
J. Phys. Chem. C XXXX, XXX, XXX−XXX